Detection of humic acid in water using flat-sheet and folded-rod viscous alkaline glucose syrups

Fakayode, O. J., Williams, S., Adekunle, A. S. & Thabo, N.

ARTICLE

Detection of humic acid in water using flat-sheet and folded-rod viscous alkaline glucose syrups

Olayemi J. Fakayode*[a], Sharon Williams[b], Abolanle S. Saheed[a] and Thabo T.I. Nkambule [a]

The utility of a low-cost biocompatible material for the detection of pollutants in water is highly essential to ensure safety and economic efficiency. In this paper, solutions of two viscous alkaline glucose syrups (AGS@22-sheet and AGS@60-rod), obtained under two different temperature conditions (22 °C and 60 °C) were used to detect low levels of humic acid (HA), a carcinogen pro-molecule and metal-complexing agent in an aqueous solution. The AGS materials were characterized using ultraviolet-visible spectroscopy (UV-Vis), Fourier transform infrared spectroscopy and scanning electron microscopy (SEM). By evaluation, a detection limit (LOD) as low as 4.6×10^{-5} mg/L was obtained. The sensing capability of the new technology was further extended to the detection of HA in a real water sample (tap water) using the standard addition method with 98 and 100.05 % recoveries. The sensing was improved in the presence of sodium acetate and sodium citrate and was found to follow a pseudo-first order reaction. These findings show that the as-synthesized glucose syrups have the potential to detect humic acid in water and thus may be employed for the quantification of HA in water treatment plants or textile industry.

Introduction

Humic acid (HA) represents one of the major fractions of natural organic matter originating from the decomposition of biological materials in water. It possesses heterogeneous structure exhibiting various functional groups such as carboxylic acid, phenolic, hydroxy, ketone, quinone, thiol and amino moieties. The presence of these groups enables HA to act as a sequestering agent for heavy metals[1–4] and aggregation platform for organic pollutants[5]. As a result of these interactions, the presence of HA in water may be undesirable for some textile or paint industries[6–8]. Also, the interaction of humic acid with chlorine in water treatment plants during water disinfection has been established as one of the routes for the formation of carcinogenic substances in water [9]. Thus, constant monitoring of levels of HA in water is highly essential to safeguard against poor product quality as well as health disorders.

Glucose is a non-toxic biocompatible and biodegradable eco-friendly carbohydrate material. In alkaline media, glucose has been reported to transform to gluconic acid and some lower carbon-chain carboxylic acids[10,11], all of which are excellent reducing agents. The production of these reducing agents will enhance the sensing capability of glucose solution, being now able to bind metal ions more easily[12–14] and form stronger organic bonds with functional groups such as carboxylic acid, phenol, thiol, alcohol and amine[15,16] under suitable conditions. Thus, exploring the potential of the alkaline glucose solution as a new sensor material may provide new information on the detection and quantification of inorganic and organic pollutants in water. It is interesting to know that while many literature reports have featured works on the detection of glucose in aqueous environments [17,18], none to the best of our knowledge has exploited the utility of glucose solution as a sensor for organic or inorganic pollutants.

Similarly, not many reports are based on the detection of humic acid in water despite the fact that it has been used to detect or as a platform for detecting other pollutants. Thus, it is of interest to evaluate the possible interaction between these two molecules. Theoretically, chemical interaction may occur between two molecules bearing different hydrophilic functional groups such as carboxylic acid, phenol, amino, hydroxy and thiol groups. This interaction may be covalent such as esterification and amide formation or non-covalent such as van der waal, hydrogen bonding and π-π aromatic stacking. Thus, a possible interaction between HA and carboxylate anion in alkaline glucose solution may involve covalent or non-covalent bonding as shown in Scheme 1.

a. Nanotechnology and Water Sustainability Research Unit (NanoWS), College of Science, Engineering and Technology (CSET), University of South Africa (UNISA), 60 Christian De Wet Street, P.O. Box 2820, Roodepoort, Florida, South Africa. Email: fakayaj@unisa.ac.za / olayemifakayode@gmail.com
b. School of Life Sciences, Faculty of Health and Life Sciences, Coventry University, 20 Whitefriars Street, Coventry, CV1 2DS, United Kingdom.
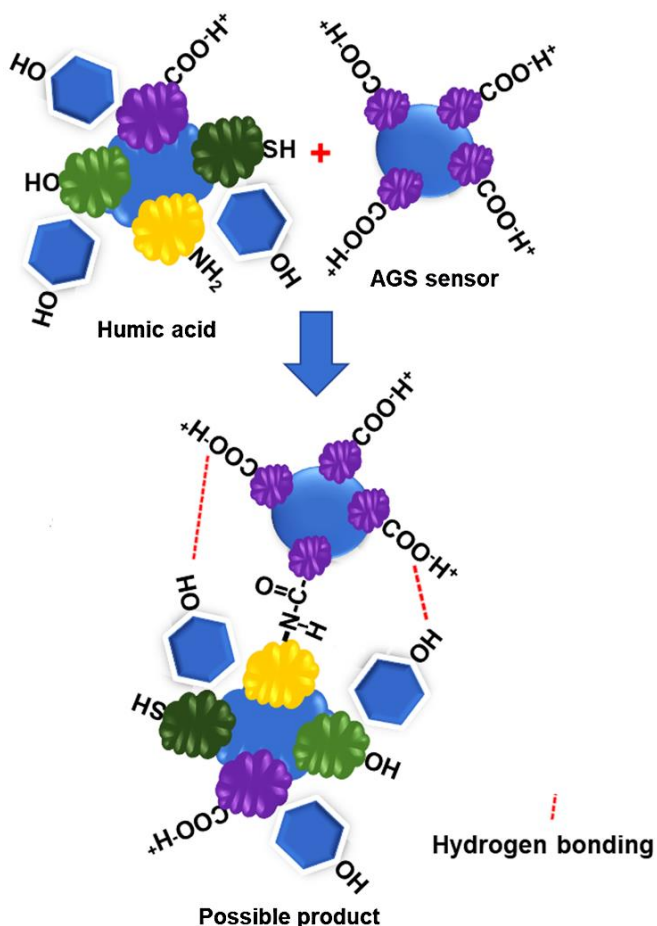
Scheme 1. Schematic diagram of the possible interaction of humic acid with alkaline glucose solution (AGS) sensor.

Conventionally, various methods for quantifying HA in water include chromatography[19], ultraviolet-visible (UV-Vis) spectrophotometry[5,20], ash-free gravimetry[21], fluorospectrophotometry (FS)[9] and total organic carbon analysis[22,23]. Among these techniques, UV-Vis has the advantage of relatively lower cost, simpler procedure and ability to provide absorption data in the ultraviolet and visible regions. The occurrence of pollutants at extremely low concentration is problematic because these pollutants may escape removal strategies such as precipitation during water treatments. Thus, fabrication of an eco-friendly sensor capable of monitoring low levels of pollutants in water is highly essential to ensure safety and better environmental sustainability. Also, fabrication of sensors using biocompatible materials at lower temperature and pressure (e.g. at room temperature conditions) is highly essential to ensure reduced cost, environmental safety and minimal energy expenditure. In this paper, solutions of viscous alkaline glucose syrups synthesized under different temperature conditions were used to quantify HA in aqueous solution. The efficacies of these materials for the

quantification of humic acid in an aqueous solution were evaluated, and the results compared with some existing reports. One of the syrups (AGS@60-rod) was used to quantify humic acid in a real water sample (tap water) using the standard addition technique.

Experimental

All materials were purchased from Sigma-Aldrich and used without further purification. Millipore ultrapure water (18 Ω. cm) was used for all aqueous preparations.

Preparation of the glucose syrups (AGS@22 and AGS@ 60)

The AGS@22 was prepared by adding equal volume of the solutions of α-(D)-glucose (anhydrous)(0.1 M) and NaOH (0.125 M)) and leaving the resulting solution in the dark, under ambient condition (room temperature: 22 ^{0}C) until a yellow solution was obtained. Some portion of this solution was dried under the ambient condition to obtain a yellow viscous solid (syrup) while another portion was left to age in the dark under ambient condition until a brown solution was obtained (Aged AGS). Similarly, the AGS@60 was obtained by heating directly the alkaline glucose solution in an oven at 60 °C until a brown viscous solid (syrup) was obtained. The latter was then cooled to the room temperature and stored until further analysis.

Detection of humic acid.

3 mL of AGS (Absorbance = 0.49192 (AGS@22) or 0.71022 (AGS@60)) was mixed with successive volumes of HA (0 - 90 μL, 0.070325 mg/L) in phosphate buffer (pH 7) and the resulting solution analyzed using the ultraviolet-visible (UV-Vis) spectrophotometry. For application in a real water sample (drinking tap water), a standard addition method was employed using the AGS@60. Briefly, a given volume of the tap water was spiked successively with a known volume of 0.2 mg/L HA in phosphate buffer solution (pH7) to obtain a final volume of 4.1 mL. Afterwards, 0.01 mL of each of the resulting solutions was added successively to 3.01 mL of AGS@60 containing 0.01 mL of tap water, followed by analysis using UV-Vis spectrophotometry.

Effect of aging, selectivity and kinetics studies

The brown AGS was used as a stock solution for the effect of aging, kinetics and selectivity studies. The brown solution was diluted with water until a light yellow solution was obtained (Absorbance = 1.0032). The latter was diluted appropriately to obtain the different final working solutions. For the effect of aging, the sensing was repeated using the same volume of HA as before (stock solution = 0.070325 mg/L) and the data compared with that of the light yellow solution before aging(AGS@22 and the AGS@60). Briefly, 2 mL of the AGS (Absorbance = 1.0032) was diluted to 3 mL using the ultrapure water (Absorbance = 0.6932, λ$_{max}$ 269 nm). Afterwards, HA in phosphate buffer solution was added successively (0-90 uL, stock solution = 0.070325 mg/L) and each resulting solution analyzed using the UV-Vis spectrophotometry. For the

selectivity studies, 2 mL of the AGS((initial absorbance = 1.0032) was diluted to 3 mL using a solution of sodium citrate(1 mL, 288.36 mg/L). The resulting solution was then subjected to the sensing procedure as above. In the case of sodium acetate, 2 mL of sodium acetate solution (65.70 mg/L) was added to 1 mL of the AGS (Initial absorbance = 1.0032) to make the final working solution. Afterwards, the sensing procedure was repeated as above. For the kinetic studies, the change in the absorbance of the AGS (Initial absorbance = 0.6932, λ_{max} = 269 nm) was monitored with time (total time = 122 s) at 269 nm for each successive addition of HA using the time drive mode of the Lambda 650s UV-Vis spectrophotometer.

Characterization

The AGS materials were characterized using ultraviolet-visible (UV–Vis) spectrophotometry (Perkin Elmer UV–Vis Lambda 650s, 2 nm slit-width spectrometer, Germany), Fourier transform infrared spectroscopy (FT-IR) (Universal Frontiers (UATR) spectrometer, Perkin Elmer, Germany), and scanning electron microscopy (SEM) (JEOL, Japan). The FT-IR ATR sample holder was pre-cleaned with 50 % ethanol and dried before sample analysis. For SEM analysis, a sample of dried AGS was placed on a black plastic tape, followed by coating with gold (5 nm, 19.32 g/cm^3) before analysis.

Results and discussion

Synthesis and characterization

The glucose solution appeared as a colourless solution after mixing with the alkaline medium. However, at about 2 h, a light-yellow solution was obtained, the intensity of which increased relatively with time under ambient conditions (22 ^{o}C). After a long aging period, the yellow solution turned brown. The occurrence of the brown colour was due to an increase in the concentration of the reducing species formed as a result of the transformation of the glucose molecule in the alkaline medium [11]. However, the yellow solution can easily be obtained from the brown solution by simply diluting the latter with an appropriate volume of water.

In the present study, the yellow solution of the alkaline glucose solution was subjected to two drying temperature conditions (22 ^{o}C and 60 ^{o}C) and the resulting viscous materials used as sensors for the detection of humic acid in an aqueous solution. The results of the SEM analysis of the AGS materials obtained from the two drying conditions are given in Fig. 1a-f. According to Fig. 1a-f, a flat-sheet morphology was obtained from the alkaline glucose solution that was dried at 22 ^{o}C while a rod-shape structure was obtained from the same solution that was dried at 60 ^{o}C. The rod exhibited an average diameter of 5.03 µm.
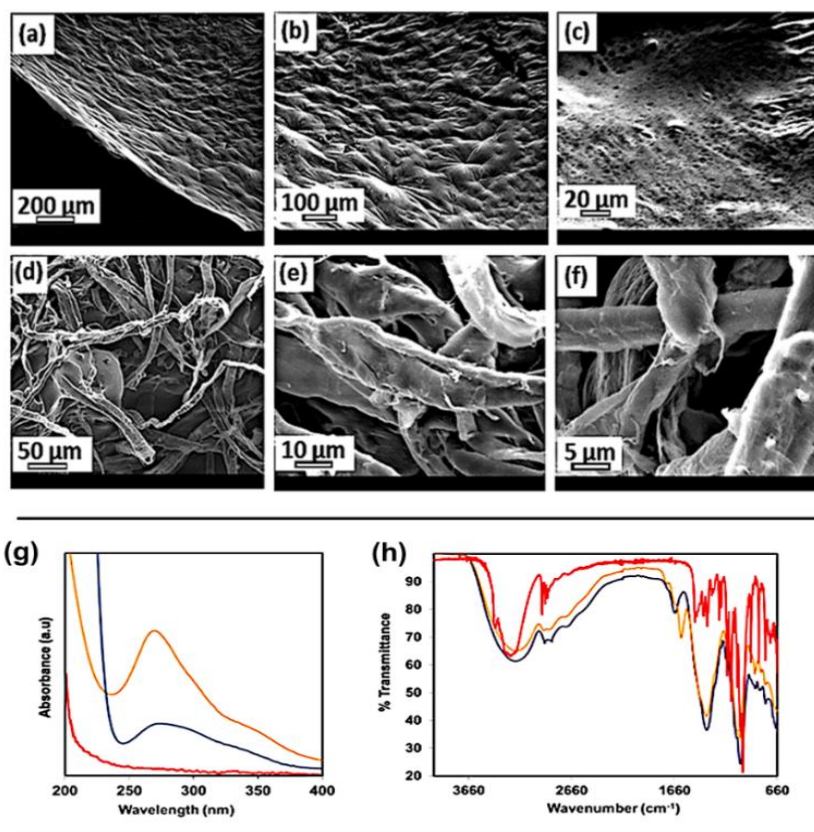
Fig. 1 Characterization of the AGS sensors. (a-c) The SEM image of the AGS dried at 22 °C at different resolutions; (d-f) The SEM image of the AGS dried at 60 °C at different resolutions; (g) UV-Vis of the aqueous solution of the AGS sensors (blue line: AGS-sheet@22; orange line: AGS-rod@60) and their precursor (α-(D)-glucose (red line)); (h) FTIR spectra of the solid AGS sensors (blue line: AGS-sheet@22; orange line: AGS-rod@60) and their precursor (α-(D)-glucose(Red line)).

The result of the UV-Vis analysis of the aqueous solutions of the two AGS materials revealed that both materials absorbed in the UV region, having major (Λ_{max}) peaks at 277 nm and 273 nm, AGS-sheet@22 and AGS-rod@60 respectively (Fig. 1g). Additionally, broader tail peaks were observed for both materials at 342 nm and 353 nm respectively (Fig. 1g). The bands of these tail peaks were responsible for the yellowish colour of the solutions of the two AGS materials [24]. In contrast, an aqueous glucose solution in the absence of the sodium hydroxide solution did not show any absorption characteristics within these regions (red line, Fig. 1g). The hypsochromic (blue) and bathochromic (red) shifts observed for the major peak and the tail-peak of the AGS-rod relative to the AGS-sheet were again seen on the FTIR's spectra of the two materials (Fig. 1h). These might be due to the effect of loss of water and thus loss of intermolecular hydrogen bonding (narrower symmetry bands of the carbonyl group (from 1743-1597, Δcm^{-1} = 146) to 1673 - 1555 (Δcm^{-1} = 118) and O-H group (from 3744-2370, Δcm^{-1} = 1374 to 3737-2390, Δcm^{-1} = 1347)) as the temperature increased from 22 °C to 60 °C) (Fig. 1h). Thus, as the rate of loss of hydrogen bonding increased, the sheet probably separated into many smaller individual sheets, which folded to become rod-like structures (Fig. 2). According to Fig. 1h, in contrast to the spectrum of the precursor (α-(D)-glucose), the presence of a carboxylic acid group was clearly seen on the spectra of the AGS materials: O-H$_{str}$ (3744-2370 broad, peak@3264 cm^{-1}), C-H$_{str}$ (2931,2894 cm^{-1}, bimodal), C-H$_{rock}$ (1365 cm^{-1}), C-O$_{str}$ (1030 cm^{-1}), C=O$_{str}$(sheet) (1663 cm^{-1}) and C=O$_{str}$(rod) (1597 cm^{-1}).

ARTICLE

22 °C

60 °C

O·H⁺

·OH

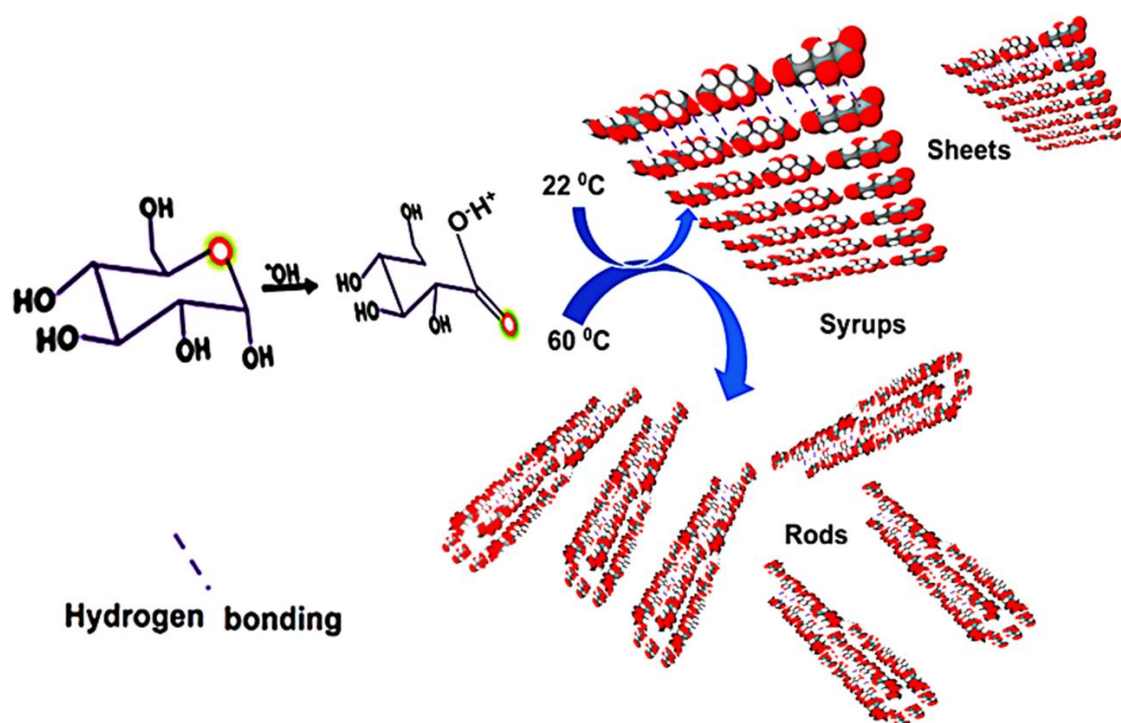Sheets

Syrups

Rods

Hydrogen bonding

Fig. 2 Schematic diagram for the formation of the AGS sheet and AGS rod at different temperatures: 22 ^{0}C and 60 ^{0}C respectively. Precursors: Glucose (0.1 M) and NaOH (0.125 M) solutions. Model, van der Waal spheres (created by Molview).

Humic acid sensing using standard calibration method

The results of the UV-Vis monitoring of the quantification of different concentrations of aqueous humic acid in phosphate buffer solution (pH 7) at different wavelengths using the AGS-sheet and AGS-rod are given in Figs. 3a-d and 4a-d respectively.

The essence of evaluating the responses at different wavelengths is to identify the wavelength with the highest absorbance (λ_{max}). This was taken to be the wavelength at which the greatest interaction occurred.
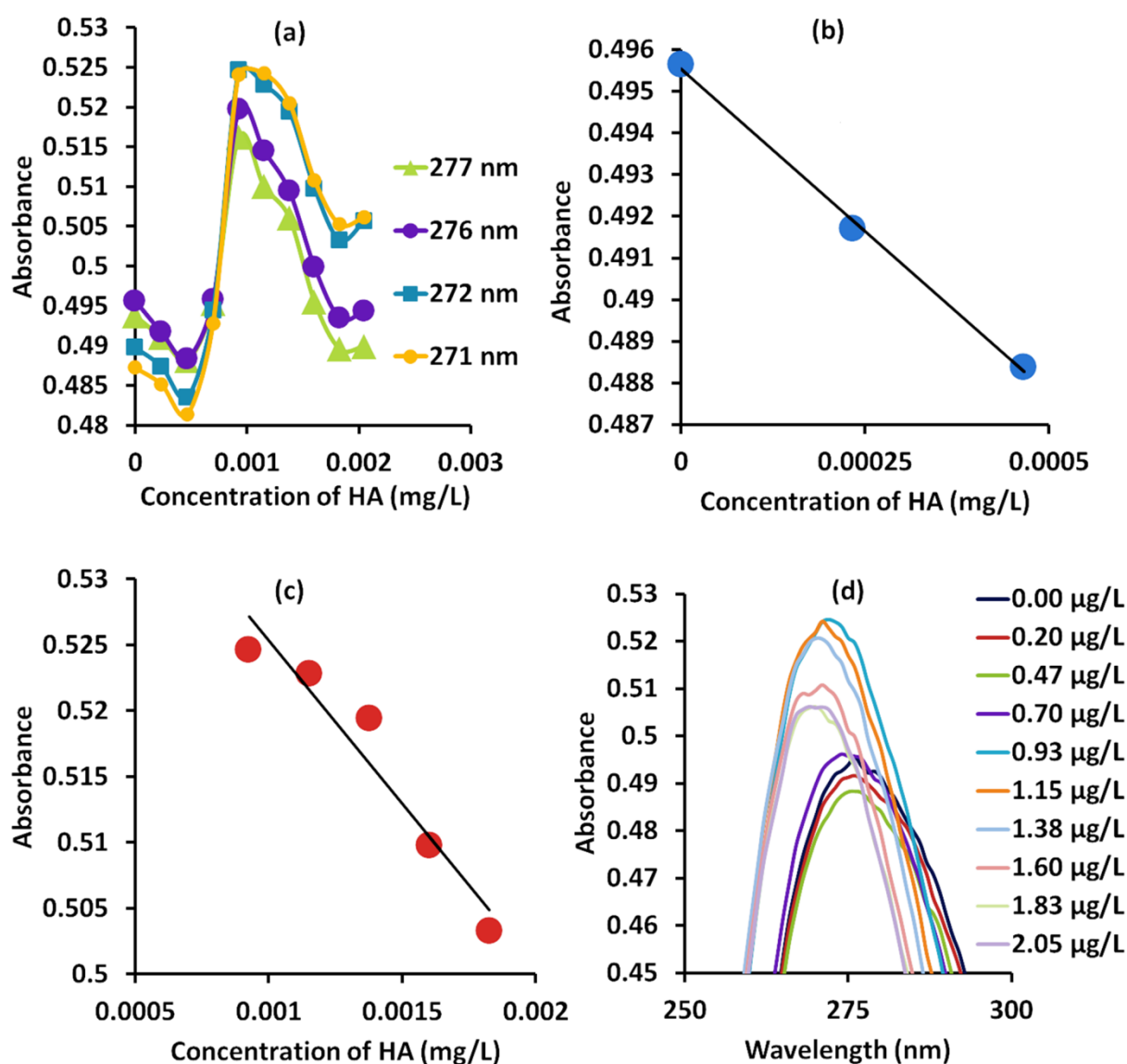
Fig. 3 Quantification of humic acid using AGS-sheet at different wavelengths (271, 272, 276 and 277 nm) over different concentration ranges. (a) 0 – 0.002048 mg/L; (b) 0 -0.00047 mg/L; (-c) 0.0009 – 0.0018 mg/L;(d)UV-Vis spectra indicating a blue shift after the addition of 0.70 µg/L of HA.
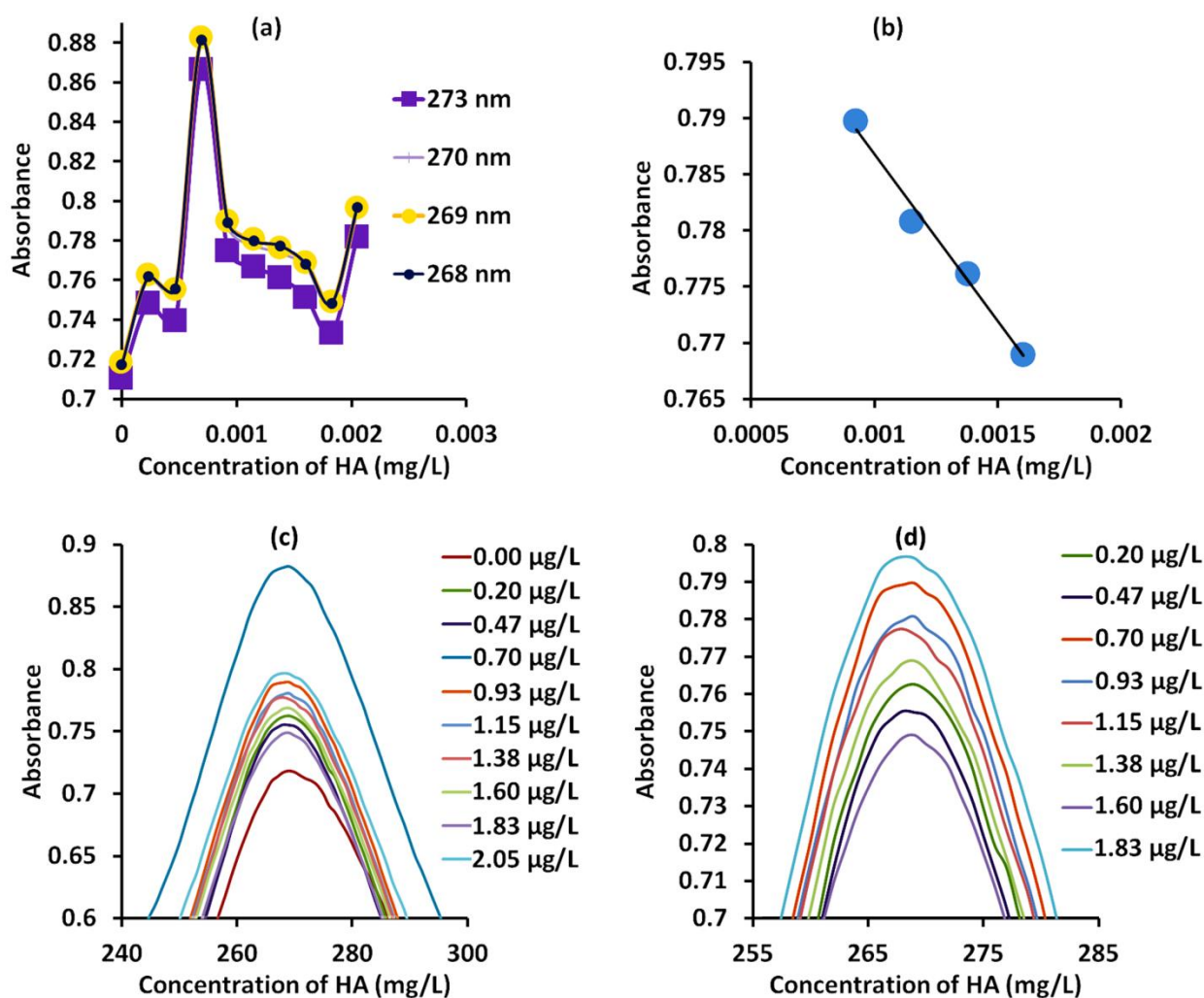
Fig. 4 Quantification of humic acid using AGS-rod at different wavelengths (268, 269, 270 and 273 nm) over different concentration ranges. (a) 0 – 0.002048 mg/L; (b) 0.0009 -0.0016 mg/L; (c) UV-Vis spectra indicating absence of a shift after the addition of HA; (d) Enlargement of the spectra associated with the 0.20-1.83 μg/L HA in (c).

According to Fig. 3a-d, two distinct linear regions can be observed for AGS-sheet, viz: 0-0.00047 mg/L and 0.0009-0.0018 mg/L. These regions were characterized with a decrease in absorbance without an obvious shift in the λ_{max}, 276 nm and 272 nm respectively. However, between these two regions, a sudden rise in absorbance (hyperchromic effect) occurred with a shift in the λ_{max} to a lower wavelength (blue shift)(Fig. 3j). This hyperchromic effect might be as a result of the increase in the concentration of the carboxylic acid groups after HA was added while the blue shift might be due to the formation of a new ground state complex[5]. In contrast, as shown in Fig. 4a-d, only

one linear region (0.0009 - 0.0016 mg/L) was observed for AGS-rod. However, similar to the AGS-sheet, this region also exhibited a decrease in absorbance without an obvious shift in the λ_{max} (269 nm). Thus, the detection limits of 4.5598 x10^{-5} mg/L and 7.318 x 10^{-4} mg/L were estimated for AGS-sheet and 3.423 x 10^{-4} mg/L for AGS-rod(Table 1). Moreover, these values were compared to some previous reports as shown in Table 1. According to Table 1, the AGS materials showed better detection limits than the literature reports. This suggests that the AGS materials have the potential for the quantification of low-level HA in aqueous solutions.

ARTICLE

Table 1 Calibration data and comparison of the present work with some existing literature

Technique	λmax (nm)	Concentration range (mg/L)	R^2	Limit of detection (mg/L)	Reference
Fluorescence	[a] 610	0 – 8	0.9972	0.4	[25]
Chemiluminescence / Ce(IV)	[a] 510 -540	0.03-10	0.9920	1×10^{-2}	[26]
FIA-Diode Array Detection	410	0-2000	0.9988	9.18	[27]
AGS-Sheet-UV-Vis[c]	276	0 – 0.00047	0.9979	4.55982×10^{-5}	
	272	0.0009-0.0018	0.9313	7.318×10^{-4}	This work
		0.0009-0.0016	0.8743	1.1415×10^{-3}	
AGS-Rod-UV-Vis[c]	269	0.0009 - 0.0016	0.9872	3.423×10^{-4}	This Work
		0.0009-0.0018	0.9223	7.8205×10^{-4}	
AGS-sheet (Aged)-UV-Vis[c]	269	0.0002 - 0.002048	0.9577	4.5×10^{-4}	This Work
AGS-sheet (Aged) + Sodium citrate-UV-Vis[c]	268	0.0000 - 0.002048	0.9778	2.15×10^{-4}	This Work
AGS-sheet (Aged) + Sodium acetate-UV-Vis[c]	268	0.0000 - 0.002048	0.9255	4.05×10^{-4}	This Work

[a]Emission wavelength; [b]NA: Data not available; FIA: Flow-injection analysis; [c]UV-Vis: Ultraviolet-visible spectrophotometry.

Effect of aging, selectivity and detection kinetics

The comparative results of the UV-Vis sensing between the room temperature aged AGS sensor and the AGS-sheet and AGS-rod are shown in Fig. S1a-c. According to Fig. S1a-c, the aged AGS (colour of the stock solution = dark brown) exhibited a different pattern of sensing from those of the AGS-sheet (colour of the stock solution = light yellow) and AGS-rod (colour of the stock solution = light yellow). Aging was described as the ability of the AGS to undergo colour change from yellow to brown after storage in the dark at room temperature. Although the initial λmax of the aged AGS was at 269 nm, similar to that of the AGS-rod, a different display of spectrum was exhibited. However, better linearity was obtained with the aged AGS compared to the AGS-sheet and AGS-rod over an extended concentration range (0.0002-0.002048)(Table 1 and Fig. S1a-c, Electronic Supplementary Information (ESI)). The reason for this might be due to the increase in the concentration of the carboxylic acid formed in the alkaline medium as the solution aged with time. This hypothesis was supported in the selectivity studies using sodium citrate (a tri-carboxylic acid molecule) and sodium acetate(a mono-carboxylic acid molecule)(Fig 5a-f,

Table 1 and Fig S2a-c, Electronic Supplementary Information (ESI)). As shown in Fig. 5a-f, Fig. S2a-c and Table 1, the presence of these molecules improved the linearity and LOD and caused the sensing range to be extended. The reason for this enhancement can be seen in the ability of these molecules to stabilize the λmax after each addition of HA, the effect being more pronounced with sodium citrate (contains 3 carboxylic acid groups per molecule) than sodium acetate (contains 1 carboxylic acid group per molecule) (Figs. S3a-c, Electronic Supplementary Information (ESI)). Typically, the stability of the λmax of a sensor after each interaction with the analyte promotes linearity and better detection limit. Moreover, to address the issue of selectivity, the sensing of the HA was enhanced over a longer concentration range rather than being impeded in the presence of these supposed to be interfering agents. In other words, both sodium citrate and sodium acetate exhibited synergetic effects with the AGS sensor by enhancing the sensing rather than interfering with the detection process. The results of the detection kinetics are shown in Fig S4a-d and Table S1 (Electronic Supplementary Information (ESI)). According to Fig. S4a, there was no significant difference in the

absorbance values obtained for each addition of HA volume (10-80 μL) over the detection period of 122 s. A relative standard deviation (RSD) of less than 0.5% was observed for each addition of HA (Table S1, Electronic Supplementary Information(ESI)). Also, repetition of measurement (n = 4) at 80 μL for the 122 s detection period showed a RSD of 0.1%(Fig. S4b, Table S1, Electronic Supplementary Information(ESI)). This shows that the analytical signals were stable for each

measurement throughout the sensing period. However, between each addition, a significant decrease in absorbance was observed(Fig. S4c, Electronic Supplementary Information(ESI)). This decrease in absorbance followed a pseudo-first order reaction as the concentration of the HA increased from $0 - 0.001827$ mg/L for the given period of detection (t = 122s)(Fig. S4d, Electronic Supplementary Information(ESI)).
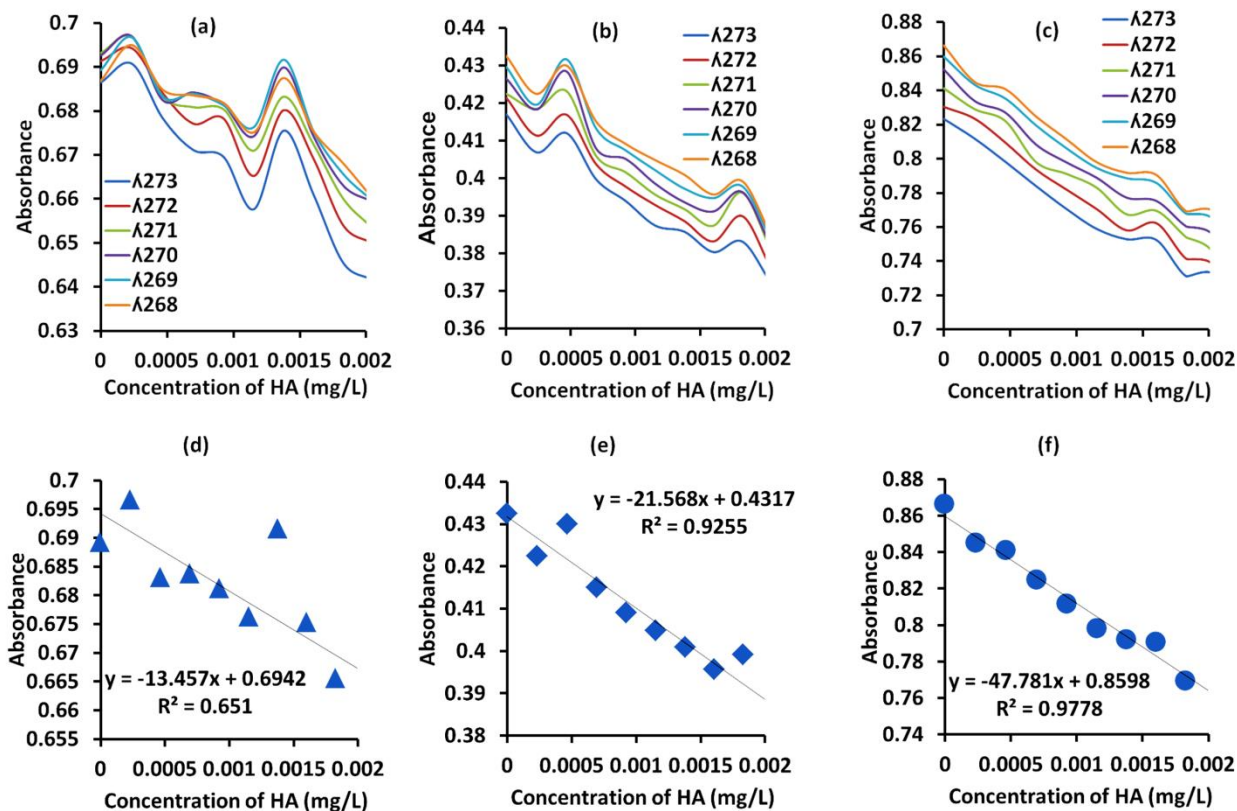
Fig. 5 Sensing of HA in the presence of sodium acetate and sodium citrate. (a,d) AGS sensor ; (b,e) AGS sensor + Sodium acetate; (c,f) AGS sensor + Sodium citrate.

Proposed mechanism of interaction

The proposed mechanism of interaction between the HA and the AGS sensors is given in Fig. 6a. Generally, the sensing range showed a decrease in absorbance as HA interacted with the AGS sensors (Fig. 3b-c and Fig. 4b). This may be due to some covalent interaction between the carboxylic acid group of the AGS and some functional amino, thiol or hydroxyl group of the HA (Fig. 6a). HA is a multifunctional compound majorly containing carboxylic acid, amino, thiol and phenolic groups (Fig. 6a). These groups may interact with the carboxylic acid group on the AGS via intermolecular hydrogen bonding or covalent bonding (e.g. ester or amide bond formation[28,29]) to cause a decrease in the absorbance of the AGS. As shown in Figs. 3d and 4c-d, a shift to a lower wavelength was associated with the AGS-sheet at some point of interacting with HA whereas no obvious shift was observed for the AGS-rod. The shift in the spectrum may refer to the formation of a new complex whose UV absorption differs entirely from the absorption of the AGS. To verify this hypothesis, the surface functional group characteristics of the AGS sensor before and after interaction with HA were compared using the FTIR technique (Fig. S5, Electronic Supplementary Information (ESI)). According to Fig. S5, a shift to a lower frequency relative to the absorption of the O-H$_{str}$ group of the carboxylic acid (Δpeak from 3300 to 3272 cm^{-1}) together with an increase in the intensity with a broader band (wider intermolecular hydrogen bonding) was evident after interaction of HA with the AGS sensor. Also, the intensities of the C=O$_{str}$ and C-O$_{str}$ were increased while that of the O-H bending decreased without any obvious shift in the wavenumber peaks. These facts not only support the

observation from the UV-Vis spectra but also indicate that the major site of interaction on the AGS material was at the O-H attached to the C=O group. This implies that interaction associated with loss of water (condensation reaction, e.g. esterification or amide bond formation) may be possible.

Similarly, the resistance of the AGS-rod to λ_{max}-shifting in the UV-Vis spectrum may indicate that the product of interaction between the HA and the AGS exhibits the same absorption characteristics as the AGS, e.g. interaction between two functional groups of relatively little or insignificant change in energy. In other words, the interaction of the AGS-sheet with HA is more energy-dependent (blue shifting) than that of the AGS-rod. This difference in property between the two AGS sensors may be explained based on the fact that more carboxylate groups may be available for interaction with HA in the sheet structure than in the rod due to a relatively wider surface configuration. This means the AGS-sheet will show stronger interactions with HA compared to the rod. This probably explains why two major linear regions (0-0.00047 mg/L and 0.0009-0.0018 mg/L) were observed for AGS-sheet and only one region (0.0009-0.0016 mg/L) for AGS-rod (Figs. 3a-c and 4a-b). However, the linearity of data (described by R^2) was higher for AGS-rod than AGS-sheet within this region, i.e. 0.0009-0.0016 mg/L, probably due to the fact that the interaction of AGS-rod was characterized by a relatively lesser energy-dependent process (Table 1). According to Table 1, this made AGS-rod exhibit a better detection limit than the AGS-sheet within this concentration range. Overall, the results in this study indicate that the approach of synthesis and thus the morphological configuration of a sensor have great impacts on the sensing capability.
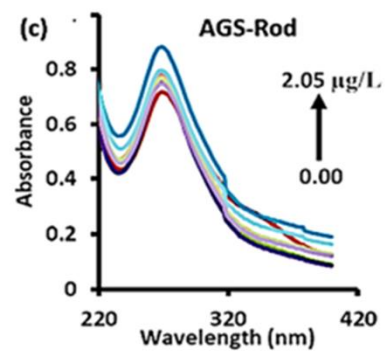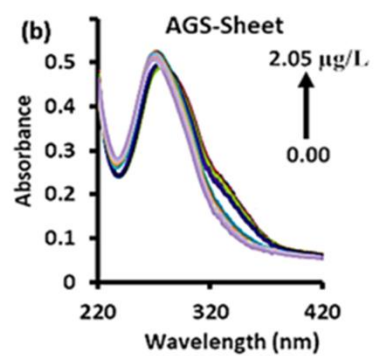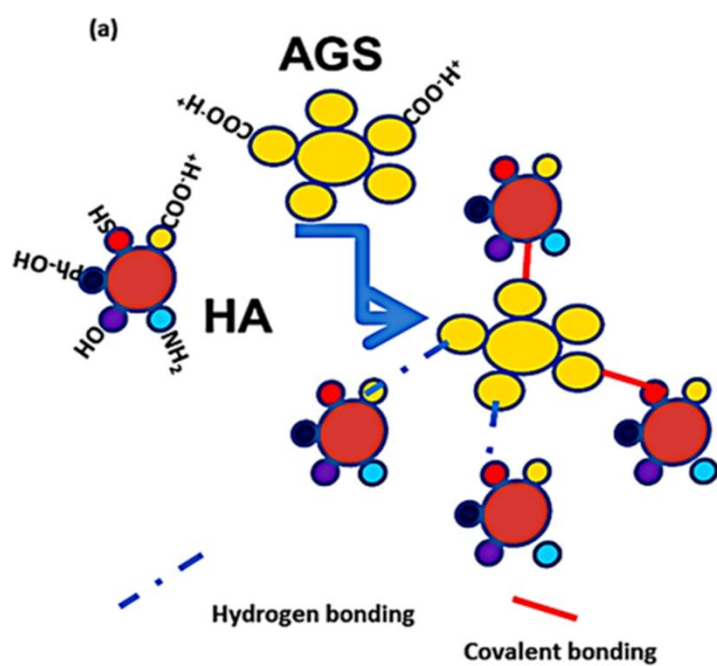
ARTICLE

Fig. 6 Interaction between AGS sensors and HA. (a) The proposed mechanism of interaction; (b) UV-Vis spectra of AGS@22 (Sheet); (c) UV-Vis spectra of AGS@60 (rod); Stock concentration of HA = 0.070325 mg/L.

Sensing humic acid in a real water sample (tap water) - standard addition method

The results of the quantification of humic acid in a real water sample (potable tap water) using the AGS-rod at 276 nm is given in Fig. 7a-b. According to Fig. 7a-b, the standard addition graph gave a straight line whose R^2 equalled to 1. Extrapolation of the straight line to the +x-axis and back-estimation using dilution factor afforded a concentration of 0.02 mg/L of HA in the tap water (Table 2). A good limit of detection of 1.20485×10^{-7} mg/L and excellent % recoveries of 98 and 100.05 were obtained (Table 2).

To verify the accuracy of the obtained concentration of HA in the tap water using the graphical standard addition technique, another technique, the standard addition estimation of the unknown using the direct mathematical relation[30] was employed (Eq. 1):

$$X_a = I_X S_F / [I_{X+S} - (I_X * V_X / V_F)] \qquad (1)$$

Where X_a = initial concentration of the analyte (HA) in the tap water, I_X = analytical signal of the tap water (absorbance of the unknown or tap water alone), S_F = final concentration of the standard, I_{X+S} = analytical signal of the (tap water + standard) or absorbance of the (unknown + standard), V_X = initial volume of the unknown (tap water) and V_F = final volume of the analytical solution. According to Table 2, the result of the estimation of HA in the tap water using the mathematical standard addition method (Eq. 1) agreed very well with the value obtained from the graphical technique. This suggests that the current sensing technology has great potential for the quantification of humic acid in real water samples.
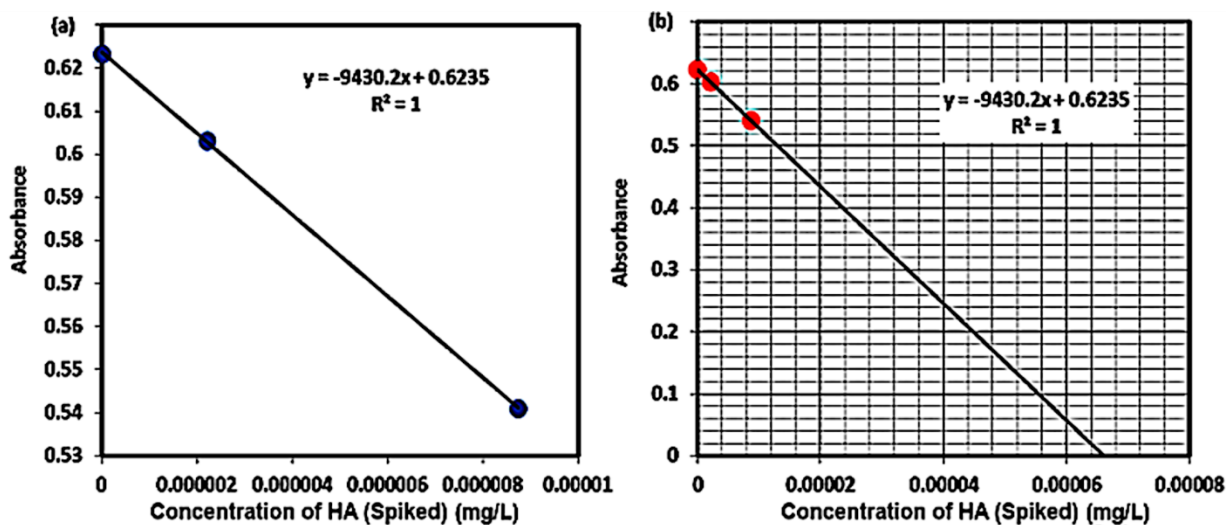

(a)

y = -9430.2x + 0.6235
R² = 1

(b)

y = -9430.2x + 0.6235
R² = 1

Fig. 7 Estimation of HA in a tap water sample using a graphical standard addition method. (a) The plot of the absorbance vs. concentration of the Spiked HA solution;(b) extrapolation of the straight line to the +x-axis.

Table 2. Estimation of HA in the tap water sample

Spiked (mg/L)	Found (mg/L)	% Recovery	Concentration (mg/L)* Graphical method	Concentration (mg/L) Mathematical method	Limit of detection[a] (mg/L)
2.20762 x 10-6	2.16803 x 10-6	98.21	0.02001	0.02287	
8.74317 x 10-6	8.74796 x 10-6	100.05	0.02021	0.02243	1.20485×10^{-7}

*volume = 10 μL; [a]LOD = 3.3 x standard deviation of intercept / slope

Conclusions

Solutions of carboxylic acid-containing alkaline glucose syrups with two morphological structures, sheet (AGS@22) and rod AGS@60), prepared under different temperature conditions (22 ºC and 60 ºC) were successfully used for the quantification of humic acid (HA) in aqueous phosphate buffer solution. Excellent detection limits were obtained for the two materials and the values were found to be better than some literature reports. On application for the quantification of HA in a real water sample (drinking tap water) using the AGS@60-rod, the estimated value of 0.02 mg/L obtained using graphical standard addition method agreed very well with value obtained using the direct mathematical estimation with excellent 98 and 100.05 % recoveries. These findings show that the as-synthesized AGS materials have the potential to be used for the quantification of humic acid in the water utility, processing and treatment sites where the presence of HA is regarded as undesirable. The present technology exhibits low-cost and energy-efficient characteristics, employs green eco-friendly biodegradable material (glucose), displays simplicity in operation and may be extended for the quantification of other organic matter's fractions in aqueous environments.

Conflicts of interest

There are no conflicts to declare.

Acknowledgements

References

1   B. Gu, C. L. Miller, W. Dong, Y. Bian, X. Jiang and L. Liang, *Proc. Natl. Acad. Sci.*, 2011, **108**, 1479–1483.
2   Z. Tang, X. Zhao, T. Zhao, H. Wang, P. Wang and F. Wu, *Environ. Sci. Technol.*, 2016, **50**, 8640–864.
3   D. Hesterberg, J. W. Chou, K. J. Hutchison and D. E. Sayers, *Environ. Sci. Technol.*, 2001, **35**, 2741–2745.
4   M. R. Esfahani, N. Koutahzadeh, A. R. Esfahani, M. D. Firouzjaei, B. Anderson and L. Peck, *J. Memb. Sci.*, 2018, **573**, 309–319.
5   X. Yuan, S. Yang, J. Fang, X. Wang, H. Ma, Z. Wang, R. W. Id and Y. Zhao, *Int. J. Environ. Res. Public Health*, 2018, **15**, 1–13.
6   A. E. Ghaly, R. Ananthashankar, M. Alhattab and V. V Ramakrishnan, *J. Chem. Eng. Process Technol.*, 2014, **5**, 1–18.
7   R. Kant, Nat. Sci., 2012, **4**, 22–26.
8   S. Madhav, A. Ahamad, P. Singh and P. K. Mishra, *Environ. Qual. Manage.*, 2018, **27**, 31–41.
9   S. Basumallick and S. Santra, *Appl. Water Sci.*, 2017, **7**, 1025–1031.
10 A. Paucean, D. C. Vodnar, V. Muresan, F. Fetea, F. Ranga, S. M. Man, S. Muste and C. Socaciu, *Acta Aliment.*, 2017, **46**, 420–427.
11 O. Novotný, K. Cejpek and J. Velíšek, *Czech J. Food Sci.*, 2008, **26**, 117–131.
12 G. M. Escandar, J. M. Salas Peregrin, M. Gonzalez Sierra, D. Martino, M. Santoro, A. A. Frutos, S. I. García, G. Labadié and L. F. Sala, *Polyhedron*, 1996, **15**, 2251–2261.
13 M. A. Amin and M. S. Refat, *Arab. J. Chem.*, 2013, **6**, 165–172.
14 O. J. Fakayode, S. P. Songca and O. S. Oluwafemi, *Sep. Purif. Technol.*, 2017, **187**, 374–379.
15 B. Gao, Y. Liu, H. Yin, Y. Li, Q. Bai and L. Zhang, *New J. Chem.*, 2012, **36**, 28–31.
16 Q. Q. Dou, C. P. Teng, E. Ye and X. J. Loh, Int. J. *Nanomedicine*, 2015, **10**, 419–432.
17 P. Chakraborty, S. Dhar, K. Debnath, T. Majumder and S. P. Mondal, *Sensors Actuators*, B Chem., 2019, **283**, 776–785.

18 X. Gu, H. Wang, Z. D. Schultz and J. P. Camden, *Anal. Chem.*, 2016, **88**, 7191–7197.
19 M. Yan, G. Korshin, D. Wang and Z. Cai, *Chemosphere*, 2012, **87**, 879–885.
20 A. Javanshah and A. Saidi, *Int. J. Adv. Biotechnol. Res.*, 2016, **7**, 19–23.
21 R. T. Lamar, D. C. Olk, L. Mayhew and P. R. Bloom, *J. AOAC Int.*, 2014, **97**, 721–730.
22 N. Kawasaki, K. Matsushige, K. Komatsu, A. Kohzu, F. W. Nara, F. Ogishi, M. Yahata, H. Mikami, T. Goto and A. Imai, *Water Res.*, 2011, **45**, 6240–6248.
23 P. Janknecht, F. Proenc and A. Rodrigues, *J. Environ. Monit.*, 2009, **11**, 377–382.
24 O. J. Fakayode, N. Tsolekile, S. P. Songca and O. S. Oluwafemi, *Biophys. Rev.*, 2018, **10**, 49–67.
25 C. Ma, M. Chen, H. Liu, K. Wu, H. He and K. Wang, *Chinese Chem. Lett.*, 2018, **29**, 136–138.
26 X. Cheng, L. Zhao, X. Wang and J. Lin, *Anal. Sci.*, 2007, **23**, 1189–1193.
27 I. Tarhan and H. Kara, *Arab. J. Chem.*, 2016, 9, 713–720.
28 H. Lundberg, F. Tinnis, N. Selander and H. Adolfsson, *Chem. Soc. Rev.*, 2014, **43**, 2714–2742.
29 T. M. El Dine, W. Erb, Y. Berhault, J. Rouden and J. Blanchet, *J. Org. Chem.*, 2015, **80**, 4532–4544.
30 D C Harris, Quantitative Chemical Analysis, Fifth Ed., Freeman and Company, USA, 2000.